

In Vivo Adjuvant-Induced Mobilization and Maturation of Gut Dendritic Cells after Oral Administration of Cholera Toxin¹

Fabienne Anjuère,^{2*} Carmelo Luci,* Michael Lebens,[†] Déborah Rousseau,* Catherine Hervouet,* Geneviève Milon,[‡] Jan Holmgren,[†] Carlos Ardavin,[§] and Cecil Czerkinsky*

Although dendritic cells (DCs) regulate immune responses, they exhibit functional heterogeneity depending on their anatomical location. We examined the functional properties of intestinal DCs after oral administration of cholera toxin (CT), the most potent mucosal adjuvant. Two CD11c⁺ DC subsets were identified both in Peyer's patches and mesenteric lymph nodes (MLN) based on the expression of CD8 α (CD8⁺ and CD8⁻ DCs, respectively). A third subset of CD11c⁺CD8^{int} was found exclusively in MLN. Feeding mice with CT induced a rapid and transient mobilization of a new CD11c⁺CD8⁻ DC subset near the intestinal epithelium. This recruitment was associated with an increased production of the chemokine CCL20 in the small intestine and was followed by a massive accumulation of CD8^{int} DCs in MLN. MLN DCs from CT-treated mice were more potent activators of naive T cells than DCs from control mice and induced a Th2 response. This increase in immunostimulating properties was accounted for by CD8^{int} and CD8⁻ DCs, whereas CD8⁺ DCs remained insensitive to CT treatment. Consistently, the CD8^{int} and CD8⁻ subsets expressed higher levels of costimulatory molecules than CD8⁺ and corresponding control DCs. Adoptive transfer experiments showed that these two DC subsets, unlike CD8⁺ DCs, were able to present Ags orally coadministered with CT in an immunostimulating manner. The ability of CT to mobilize immature DCs in the intestinal epithelium and to promote their emigration and differentiation in draining lymph nodes may explain the exceptional adjuvant properties of this toxin on mucosal immune responses. *The Journal of Immunology*, 2004, 173: 5103–5111.

Mucosae are continually exposed to potentially antigenic molecules. The mucosal immune system discriminates between pathogenic microorganism-derived molecules and inflammatory inert molecules: as a result, either immune responses against potential pathogens or a state of systemic unresponsiveness (also called oral tolerance) against innocuous Ags is induced. If properly regulated, these processes contribute to generate tightly controlled inflammatory processes with antimicrobial properties or to prevent tissue-damaging inflammatory responses from occurring (1, 2).

To give rise to protective immunity to a given pathogen, mucosal vaccines require the use of adjuvants that will override the natural bias of the mucosal immune system toward the induction of

tolerance. Cholera toxin (CT),³ one of the most potent mucosal adjuvants, when coadministered with foreign Ags not only abrogates oral tolerance but also potentiates predominantly Th2-type responses and B cell responses (3–6).

CT has an AB₅ structure composed of two distinct structural and functional subunits: a single toxic A subunit and a nontoxic cell-binding B subunit homopentamer (CTB) with strong affinity for GM1 ganglioside (7), which is present on all mammalian nucleated cells. Although the mucosal adjuvant properties of CT are well documented and are associated with its A subunit, the cellular mechanisms involved in CT-mediated promotion of Th2 cell development remain poorly understood.

Dendritic cells (DCs) constitute unique APCs, described to play a major role in both induction of immunity and tolerance (8). In most nonlymphoid tissues, DCs act as sentinels, sampling Ags and then migrating to secondary lymphoid organs where they initiate specific immune responses (9). Murine DCs can be subdivided on the basis of CD8 α expression. Thus, CD8⁻ and CD8⁺ DC subpopulations are present in most lymphoid organs and interstitial tissues. Moreover, DCs expressing intermediate levels of CD8 (CD8^{int} DCs) constitute a lymph node-specific subset, which gain access to the LNs via lymphatics (10). In peripheral lymph nodes, CD8^{int} DCs appear to derive from epidermal Langerhans cells (LCs) and perhaps from dermal DCs (10, 11). The precursors of CD8^{int} mesenteric lymph node (MLN) DCs remain to be identified. Because the site of DC development influences DC function (12), we have examined the compartment of DC subsets in gut-associated lymphoid tissues after intestinal immunization with CT.

*Institut National de la Santé et de la Recherche Médicale, Nice, France; [†]Department of Medical Microbiology and Immunology, and Göteborg University Vaccine Institute, Göteborg, Sweden; [‡]Pasteur Institute Immunophysiology and Intracellular Parasitism Unit, Paris, France; and [§]Department of Immunology and Oncology, National Center for Biotechnology, Madrid, Spain

Received for publication November 7, 2003. Accepted for publication August 10, 2004.

The costs of publication of this article were defrayed in part by the payment of page charges. This article must therefore be hereby marked *advertisement* in accordance with 18 U.S.C. Section 1734 solely to indicate this fact.

¹ These studies were supported by the European Union (6th Programme Cadre de Recherche et Développement), Institut National de la Santé et de la Recherche Médicale (France), Fondation pour la Recherche Médicale (France), Direction Générale des Armées (France), Swedish Medical Research Council, Triotol AB (Sweden), and Gothenburg University Vaccine Research Institute (Sweden). G.M. acknowledges the funding of Institut Pasteur as well as the funding of Centre National de la Recherche Scientifique (appel d'offres puces à Acide Desoxyribonucleique co-Principal Investigators Pages/Glaser and Milon).

² Address correspondence and reprint requests to Dr. Fabienne Anjuère, Institut National de la Santé et de la Recherche Médicale E-0215, Institut Fédératif de Recherche 50, Faculté de Médecine Pasteur, Avenue de Valombrose, 06107 Nice cedex 2, France. E-mail address: anjuere@unice.fr

³ Abbreviations used in this paper: CT, cholera toxin; DC, dendritic cell; LC, Langerhans cell; int, intermediate; MLN, mesenteric lymph node; HA, hemagglutinin; HEV, high endothelial venule; PP, Peyer's patch; IE DC, intestinal epithelial DC; RT, room temperature; PERFEXT, perfusion-extraction; RPA, RNase protection assay.

Our data demonstrate that feeding CT induces a rapid mobilization of immature DCs in the intestinal wall, which is followed by the expansion of more mature DCs in draining MLNs. More importantly, specific subsets of DCs from MLN are able to present Ags coadministered orally with CT and display enhanced T cell-stimulatory properties. These results further explain the exceptional adjuvant properties of CT and provide a cellular basis for CT-mediated immune responses induced at mucosal surfaces.

Materials and Methods

Animals and oral immunizations

Female BALB/c mice (Charles River Laboratories, L'Arbresle, France), aged 6–8 wk, were used in all experiments. TCR-HA transgenic BALB/c mice expressing the 14.3.d. HA-specific TCR, which recognizes the hemagglutinin (HA) epitope from influenza virus HA (HA_{110–119}) in association with I-E^d (13) were a kind gift from Dr. H. von Boehmer (Harvard, Cambridge, MA). Mice were given 10 μ g of CT in 500 μ l of 3% NaHCO₃ administered by intragastric intubation with a feeding needle (Harvard, Holliston, MA). In some experiments, mice were fed 150 μ g of CTB:HA gene fusion protein in the presence or absence of 10 μ g of CT. Blocking of CT-induced blood cell migration via high endothelial venules (HEVs) in MLNs was achieved by i.v. injection of 100 μ g of purified anti-CD62L (clone MEL-14; BD Pharmingen, San Diego, CA), purified anti- $\alpha_4\beta_7$ (clone DATK32; BD Pharmingen), or purified isotype control (rat IgG2a; clone R35-95) mAbs twice 24 and 1 h before feeding CT to a dose shown efficient to block migration from blood.

CTB-Ag conjugates and peptides

Purified CT was obtained from List Biologicals (Campbell, CA). The HA:CTB fusion protein was obtained by insertion of a double-stranded synthetic oligonucleotide (obtained from Innovagen, Lund, Sweden) encoding the HA peptide into the plasmid expression vector pML-LCTB λ 7 (a derivative of pML-LCTB λ 2 (14) carrying the *ctxB* gene under the control of the powerful λ P₁ promoter). The oligonucleotide was inserted such that the HA peptide was fused to the N terminus of mature CTB. The modified gene also encoded the *heltB* signal peptide sequence directing the secretion of the expressed protein into the periplasmic space. The fusion protein was expressed in *Escherichia coli* strain N3480-1, a λ lysogen containing the temperature-sensitive *cI₅₈₇* repressor. Cultures were grown in Luria-Bertani broth at 30°C until they had reached early log phase. Expression was then induced by increasing the culture temperature to 42°C and continuing to grow the cells for a further 3–4 h. The cells were harvested by centrifugation, and periplasmic preparations were made by treatment with lysozyme in conjunction with osmotic shock (15). The protein was purified by precipitation using hexametaphosphate and redissolving in PBS followed by further purification by gel filtration. The HA peptide (SVSSFERFEIFPK) was obtained from Neosystem (Strasbourg, France).

Adoptive transfer experiments

A total of 5×10^4 DCs was injected s.c. in the footpad of transgenic TCR-HA BALB/c mice. Seven days later, the draining lymph nodes were excised and analyzed.

DC isolation

DCs were purified from MLN and Peyer's patches (PP), adapting a protocol previously described (10, 16). Briefly, organs fragments were digested with collagenase A (Boehringer-Mannheim, Mannheim, Germany) and DNase I (Boehringer-Mannheim) in RPMI 1640 medium supplemented with 5% FCS, filtered through a stainless-steel sieve, and cell suspensions were washed twice in PBS solution supplemented with 5% FCS and 5 mM EDTA (PBS-EDTA-FCS) containing 5 μ g/ml DNase I. The cell suspensions were then enriched in low-density cells by centrifugation in cold iso-osmotic Optiprep solution (Nyegaard Diagnostics, Oslo, Norway) (pH 7.2; density, 1.061 g/cm³). Unwanted contaminating B and T cells were removed magnetically after sequential incubation for 30 min at 4°C with anti-CD3 (clone KT3-1.1) and then with a 1:1 mixture of anti-mouse Ig- and anti-rat Ig-coated magnetic beads (Dynabeads; Dynal, Oslo, Norway) at a 7:1 bead-to-cell ratio according to the manufacturer's instructions. In functional experiments, DCs were then enriched by positive selection using anti-CD11c magnetic beads and cell sorting with MACS separation columns (Miltenyi Biotec, Bergisch, Germany) according to the manufacturer's recommendations. The DC preparations obtained by this technique had a purity of >95% and contained no detectable CD3⁺ or TCR β ⁺ cells. DC subsets were fractionated by cell sorting of highly pu-

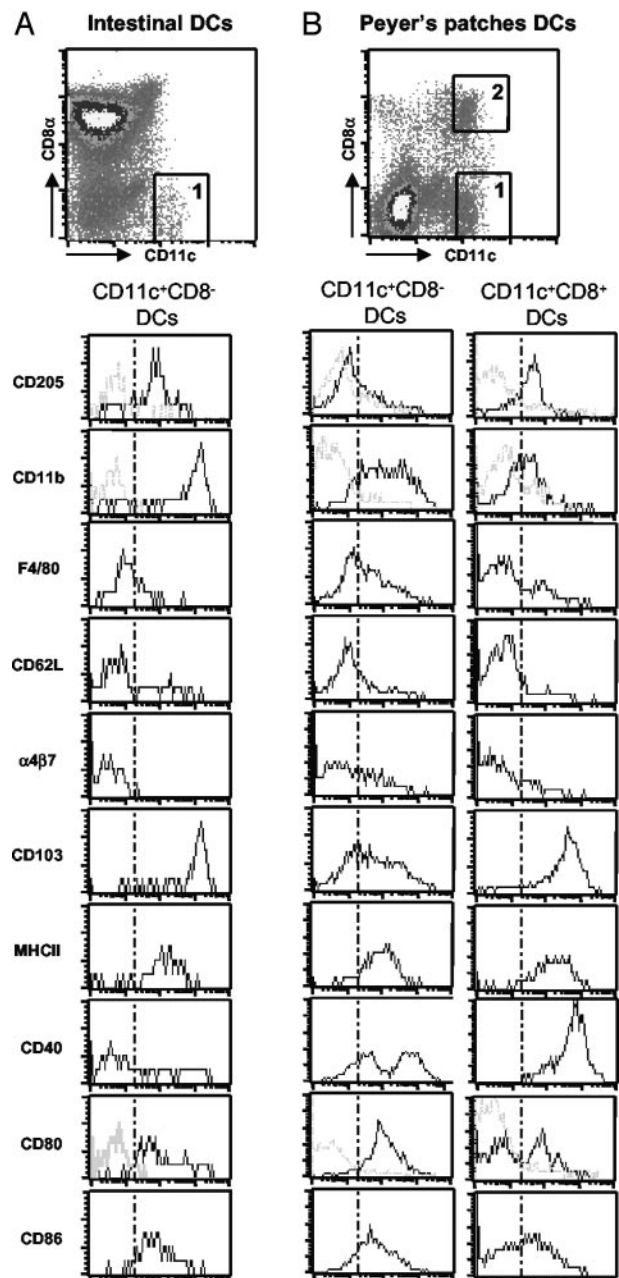


FIGURE 1. Phenotype of mouse CD11c⁺ DCs from the small intestine mucosa. *A*, Flow cytometry analysis of cell suspensions isolated by EDTA/DTT dispersion of small intestines from normal BALB/c mice. Dark-line histograms represent expression of different markers for gated CD11c⁺CD8⁻ cells (gate 1) corresponding to intestinal CD11c⁺ DCs. *B*, Flow cytometry analysis of CD11c⁺ PP DCs. Histograms represent expression of different markers for gated CD11c⁺CD8⁻ cells (gate 1) and for gated CD11c⁺CD8⁺ cells (gate 2). In both analyses, light-gray histograms overlaying CD205, CD11b, and CD80 histograms represent the three different isotype controls used. In the other histograms, dashed vertical lines corresponding to the upper limit of isotype control background staining are indicated.

riated DC preparations using a FACSVantage cell sorter (BD Biosciences, Mountain View, CA) after triple staining as described in flow cytometry (see below).

Intestinal epithelial DCs (IE DCs) were purified from small intestine fragments after removal of detritus and PP using a procedure adapted from a protocol for isolation of intraepithelial lymphocytes. Small intestine pieces of 5 mm were incubated for 30 min at room temperature (RT) in 50 ml of RPMI 1640 supplemented with 5 mM EDTA, 2 mM DTT, and 2%

horse serum (Invitrogen Life Technologies, Paisley, Scotland). The cells in the supernatant were washed once in RPMI 1640 supplemented with 5 mM EDTA and 5% horse serum and then resuspended in cold iso-osmotic Optiprep solution (Nyegaard Diagnostics) (pH 7.2; density, 1.040 g/cm³), loaded onto an Optiprep solution at a density of 1.059 g/cm³ and centrifuged for 10 min at 1700 × *g*. The cells at the interface of both densities were recovered and washed twice in PBS-EDTA-FCS. Such cell suspension contained ~0.5–1% of CD11c⁺ cells as determined by flow cytometry analysis and was used for IE DC phenotype analysis.

Proliferation assay

In some experiments, HA-specific proliferative responses from cells previously primed by *in vivo* injection of DCs were determined on triplicate cultures of lymph node cell suspensions. Cells were seeded at 2 × 10⁵ cells per flat-bottom well of 96-well culture plates (Falcon; BD Biosciences) in the presence or absence of HA peptide (10 μg/ml). In other experiments, graded numbers of purified MLN DCs or PP DCs from control or CT-fed mice were cultured with CD4⁺ naive T cells from TCR-HA transgenic mice (2 × 10⁵) in the presence or absence of HA peptide (10 μM). After incubation at 37°C for 72 h, cultures were pulsed for another 18-h period with 1 μCi of [³H]thymidine. Cultures were harvested onto glass-filter harvester, and the extent of radioactive thymidine incorporated was measured with a beta scintillation counter.

T cell polarization assay

Purified MLN DCs (10⁴) from control or CT-fed mice were cultured with CD4⁺ naive T cells from TCR-HA transgenic mice (2 × 10⁵) in the presence or absence of HA peptide (10 μM). HA-experienced T cells were harvested after 48 h and subsequently cultured with 10⁵ accessory cells. Syngeneic BALB/c spleen cells pulsed 1 h with HA peptide (10 μM) at 37°C and washed were used as accessory cells. Culture supernatants from these secondary cultures were assayed for IFN-γ, IL-4, IL-5, and IL-10

contents using ELISA kits (Duoets; R&D Systems, Abingdon, U.K.), according to the manufacturer's instructions. Briefly, high binding 96-well polystyrene plates (Nunc, Roskilde, Denmark) were coated with 100 μl of either anti-IL-2, IFN-γ, IL-4, and IL-5 coating Abs (2 μg/ml) in 0.1 M phosphate buffer overnight at RT followed by a step of saturation of 60 min in 1% nonfat milk powder with 0.12% Triton X-100. All steps were performed at RT and followed by three washes with PBS containing 0.05% Tween 20 (PBST). Supernatants were diluted 2- to 5-fold in PBST with 1% nonfat milk and incubated for 2 h at RT. After washing, the wells were exposed for 1 h to biotinylated Abs to IL-2, IFN-γ, IL-4, or IL-5 (0.1 μg/ml) in PBST, and developed by stepwise addition of streptavidin-biotinylated HRP complex (ABC avidin/biotin complex; Amersham Biosciences, Piscataway, NJ) and 3,3',5,5'-tetramethyl benzidine/H₂O₂ (Kirkegaard and Perry Laboratories, Gaithersburg, MA).

Immunohistochemistry

Mice were sacrificed at various times after feeding with CT. Small fragments of duodenum and jejunum devoid of macroscopic PP were rinsed thoroughly with tap water and fixed overnight at 4°C in Tris-calcium acetate buffer containing zinc acetate (0.5%) and zinc chloride (0.5%). Specimens were dehydrated in solutions of acetone (70 and 100%) and embedded in low melting point (37–39°C) paraffin wax (BDH Laboratories, Poole, U.K.) (17). Serial 10-μm sections were prepared and dried overnight at RT onto glass microscope slides (Superfrost Plus; Kindler, Freiburg, Germany). Before staining, slides were dewaxed in acetone for 3 min, washed with PBS, and exposed to 10% FCS diluted in PBS for 30 min at RT. Sections were then incubated with biotin-conjugated anti-CD11c mAb (clone N418; homemade) (1 μg/ml) or with biotin-conjugated polyclonal Armenian hamster IgG isotype Abs (BD Pharmingen) at the same concentration for 1 h at RT. Specific binding was revealed after incubation during 30 min with ABC-HRP complex (Amersham Biosciences) followed

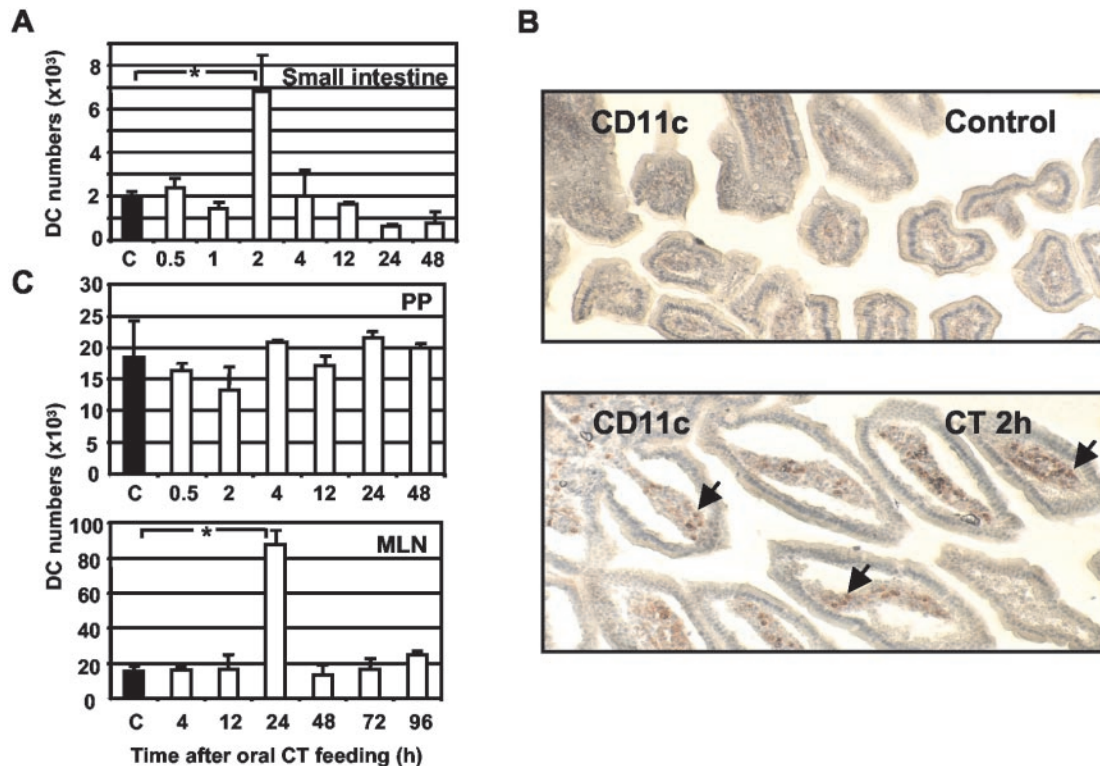


FIGURE 2. Increased numbers of DCs in both the mouse small intestine epithelium and the MLN following oral administration of CT. *A*, Cell suspensions from small intestine were prepared from control (■) and CT-fed (□) BALB/c mice at different intervals after feeding CT. DC numbers were determined after counting viable cells and analysis of CD11c⁺CD8[−]MHCII⁺ DC percentage after triple staining with FITC-conjugated anti-CD11c, PE-conjugated anti-CD8α, and biotin-conjugated anti-MHCII followed by streptavidin tricolor. Results are expressed as means (+SEM) DC numbers per small intestine (*n* = 5 independent experiments). *, Significant difference (*p* < 0.05; Student-Newman-Keuls test). *B*, Immunohistochemical localization of CD11c⁺ cells in transverse sections of small intestine fragments from control mice or from mice 2 h after feeding CT. Sections were counterstained with H&E. Note the characteristic atrophy of villi in CT-treated mice. The majority of stained cells (arrows) are located in the subepithelial region of the villi (magnification, ×200). *C*, DCs from MLN and PP were isolated at different time points after feeding CT (□) or not (■). DC numbers were determined by counting purified DC cells and represent means (+SEM) from six independent experiments. *, Significant difference (*p* < 0.001, Student-Newman-Keuls test).

by incubation with chromogen substrate (3-amino-9-ethylcarbazole and H_2O_2). Slides were counterstained with H&E.

Flow cytometry

Phenotypic analysis of DCs was performed after triple staining with FITC-conjugated anti-CD11c (clone N418), PE-conjugated anti-CD8 α (clone 53-6-7; BD Pharmingen), and biotin-conjugated anti-CD11b (clone M1/70; Caltag Laboratories, San Francisco, CA), anti-MHCII (clone 2G9; BD Pharmingen), anti-CD103 ($\alpha_E\beta_7$) (clone M290; BD Pharmingen), anti-CD80 (clone 16-10A1; BD Pharmingen), anti-CD86 (clone GL1; BD Pharmingen), anti-CD40 (clone 3/23; BD Pharmingen), anti-CD205 (clone NLDC-145; Cedarlane Labs, Hornby, Ontario, Canada), anti-CD3e (clone 145-2C11; BD Pharmingen), anti-TCR β (clone H57-597; BD Pharmingen), or anti-macrophage F4/80 (clone C1.A3-1; Caltag Laboratories) followed by streptavidin-tricolor (Caltag Laboratories). Biotin-conjugated rat IgG2a (clone R35-95; BD Pharmingen), rat IgG2b (clone A95-1; BD Pharmingen), and hamster IgG1 (clone A19-3; BD Pharmingen) IgG2 (clone B81-3; BD Pharmingen) were used as isotype controls. Before specific staining, cell surface FcRs were blocked by incubation with purified anti-Fc γ RII/III mAb 2.4G2 (BD Pharmingen). All staining steps were performed at 0–4°C in PBS containing 5 mM EDTA and 3% FCS. Analyses were performed on a FACScan flow cytometer (BD Biosciences) at the Flow Cytometry Laboratories of Institut Fédératif de Recherche 50 (Faculty of Medicine, Nice, France) using CellQuest software (BD Biosciences). The sorting of DC subsets was performed after triple staining with FITC-conjugated anti-CD11c (clone N418), PE-conjugated anti-CD8 α (clone 53-6-7; BD Pharmingen) and tricolor-conjugated anti-CD11b (clone M1/70; Caltag Laboratories) on a FACS Vantage cytometer using CellQuest software (BD Biosciences). FACS analyses of lymph node CD4⁺TCR-HA⁺ T cells were performed after double staining with FITC-conjugated anti-TCR-HA clonotypic Ab (clone 6.5; a kind gift from Dr. H. von Boehmer) and PE-conjugated anti-CD4 (clone CT-CD4; Caltag Laboratories).

RNA extraction and RNase protection assay (RPA)

Liquid nitrogen frozen fragments of small intestine tissues devoid of PP were immediately ground in RNable solution (Eurobio, Les Ulis, France) (1 ml/50 mg of tissue). RNAs were prepared according to the manufacturer's instructions, analyzed on a 1% agarose gel, quantitated by spectrometry, and stored at –80°C until use. The amount of different chemokines, GAPDH, and L32 mRNAs was estimated by RiboQuant RPA using a customized template set (BD Pharmingen) and according manufacturer's instructions. Briefly, riboprobes were labeled with ³²P and hybridized overnight in solution with RNA (15 μ g). The hybridized RNA was digested with RNase, and the remaining RNase-protected probes were purified, resolved on denaturing polyacrylamide gels, and imaged by autoradiography according to the RiboQuant protocol. The RNA transcript levels were determined by reference to internal control signals (GAPDH and L32), and the results were expressed in arbitrary units.

Detection of chemokines in intestinal tissues

Detergent-solubilized intestinal tissues were prepared after perfusion of mice under general anesthesia, according to the perfusion-extraction (PERFEXT) method (18) with minor modifications. Mice received an i.p. injection of heparin (1500 U/ml; Sigma-Aldrich, St. Louis, MO) in PBS. Animals were bled through the carotid vein and subsequently perfused with 10 ml of heparin-PBS (150 U/ml) and 20 ml of PBS through the heart to remove contaminating blood from tissues. The small intestine was removed, and 2-cm-long fragments were prepared from the duodenum and the jejunum and further perfused ex vivo with PBS containing heparin (150 U/ml). Specimens were blot dried, weighed, suspended in extraction buffer (10 ml/mg of tissue), and immediately frozen in liquid nitrogen. The extraction buffer consisted of 0.01 M PBS with containing 1% (v/v) Complete protease inhibitor mixture (Roche Applied Science, Penzberg, Germany), and 90 mM CHAPS (Research Organics, Cleveland, OH). The samples were allowed to thaw overnight at 4°C and spun down at 13,000 \times g, and supernatants were analyzed for MIP-3 α /CCL20 levels by ELISA using a mouse MIP-3 α /CCL20 kit (Duoset; R&D Systems) according to the manufacturer's instructions. MIP-3 α /CCL20 concentrations were determined by reference to a standard curve generated by assaying known amounts of chemokine.

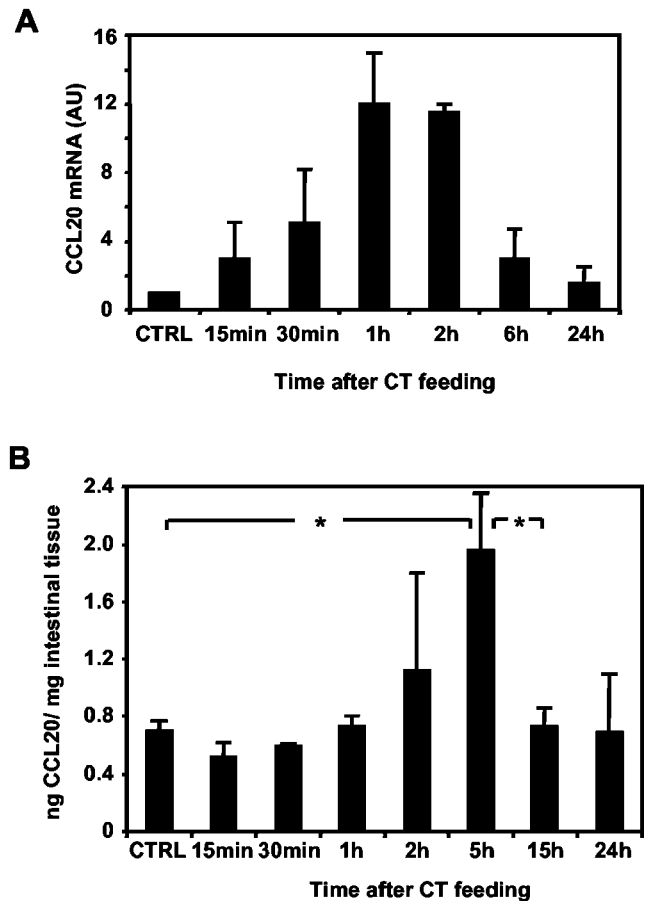


FIGURE 3. Oral administration of CT up-regulates the expression of the chemokine CCL20/MIP3 α by intestinal tissue. **A**, Levels of expression of MIP-3 α /CCL20 mRNA were determined by RPA on intestinal tissue specimens from mice fed CT at different time points. Data are expressed in arbitrary units by reference to a value of 1 assigned to control specimens from unfed mice. Data represent mean values (+SEM) from three independent experiments. **B**, Levels of MIP3 α /CCL20 protein were determined by ELISA on intestinal tissue specimens processed by the PERFEXT technique. Results are expressed as means (+SEM) of four independent experiments. *, Statistical difference ($p < 0.05$ Student-Newman-Keuls test).

Results

Oral administration of CT induces a rapid accumulation of immature DCs in intestinal mucosa

We first isolated DCs present in the murine small intestine. Preliminary studies indicated that the vast majority of intestinal DCs could be released from fragments of the small intestine by simple mechanical dispersion in the presence of EDTA and DTT, suggesting they were in close contact with the epithelium. This initial step, classically used for extraction of epithelial cells and intraepithelial lymphocytes, was followed by an enrichment of low-density cells, yielding a cell suspension in which ~1% of nucleated cells expressed CD11c (corresponding to 1700 ± 600 DCs per small intestine). As shown in Fig. 1, these CD11c⁺ cells, referred to hereafter as IE DCs, express intermediate levels of MHCII and low levels of costimulatory molecules CD80, CD86, and CD40, suggesting that they constitute an immature DC subset. They are positive for CD11b and DEC-205 but are negative for CD8 α and CD62L and the integrin $\alpha_4\beta_7$. This phenotype is strikingly similar to skin LCs (data not shown). However, unlike LCs, IE DCs strongly express the integrin CD103 ($\alpha_E\beta_7$) and express very low

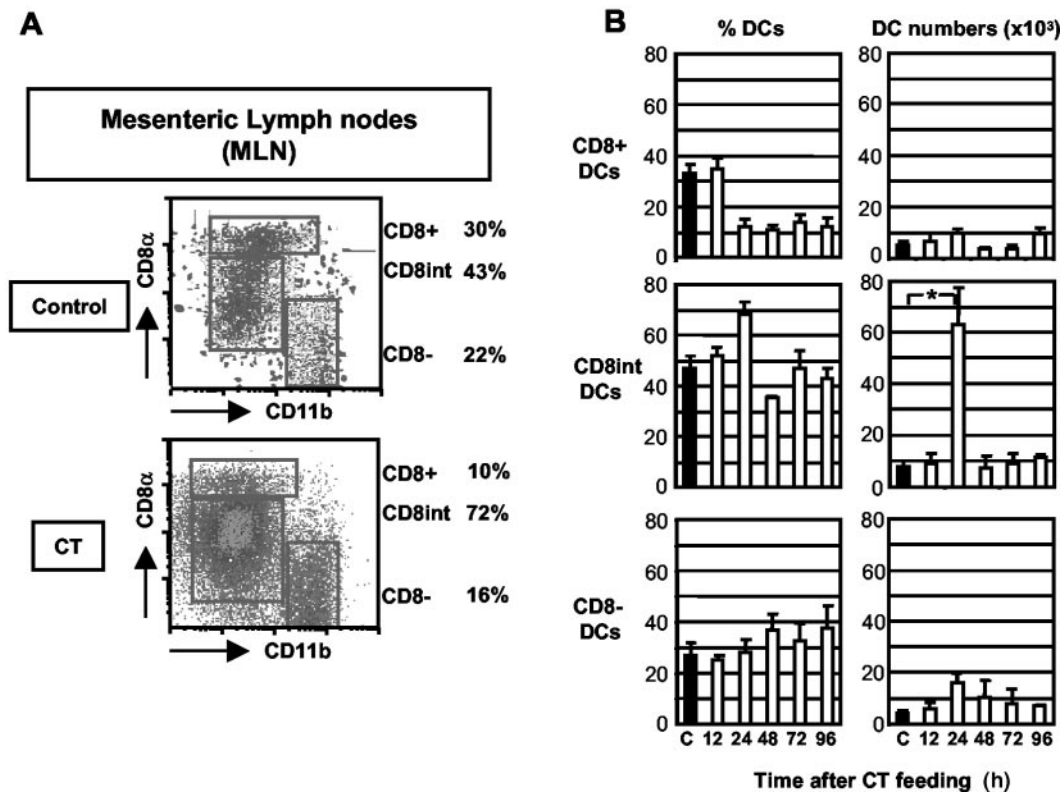


FIGURE 4. Oral administration of CT induces selective expansion of CD8^{int} DCs in MLN. *A*, DCs isolated from MLN from mice 24 h after oral administration of CT or from control mice were analyzed by flow cytometry after triple staining using FITC-conjugated anti-CD11c, PE-conjugated anti-CD8 α , and biotin-conjugated anti-CD11b followed by streptavidin tricolor. Contour plots show CD8 α vs CD11b staining of gated CD11c⁺ cells corresponding to DCs, which represent >85% of total cells. *B*, Bars correspond to the means (+SEM) of relative percentages and absolute DC numbers in the MLN CD8⁺, CD8^{int}, and CD8⁻ DC subsets, in control mice (■) and treated mice at the indicated times after CT feeding (□) from six independent experiments. *, Significant difference ($p < 0.001$, Student-Newman-Keuls test).

levels of the macrophage marker F4/80. Furthermore, as shown in Fig. 1, IE DCs have a phenotype different from PP DC subsets.

We then tested the effect of oral administration of CT on IE DC numbers. As shown in Fig. 2*A*, 2 h after feeding CT, 4-fold more IE DCs were isolated from the small intestine of CT-treated mice ($n = 5$ experiments; range, 5,700–11,000) as compared with control mice ($n = 5$; range, 1,100–2,300). This increase in IE DC numbers after CT treatment was transient; 4 h after feeding CT, IE DC numbers had returned to baseline levels. Transverse sections of small intestine obtained 2 h after feeding CT disclosed CD11c⁺ cells scattered beneath the villus epithelium, whereas such CD11c⁺ cells were barely detectable in control mice (Fig. 2*B*). Oral CT did not affect the levels of costimulatory molecules CD80, CD86, and CD40 or MHCII expression by IE DCs (data not shown).

Because DCs from PP are also located in close contact with the intestinal lumen, we evaluated the effect of oral administration of CT on the frequency of PP DC subsets. PP DCs were purified from mice at different time points after feeding with CT and compared with DCs obtained from control mice. As shown in Fig. 2*C*, oral administration of CT had no appreciable effects on the numbers of DCs isolated from PP at all times examined between half an hour and up to 48 h.

Oral administration of CT up-regulates MIP-3 α expression by intestinal epithelial cells

To examine whether the modulation of expression of certain chemokines could explain the rapid recruitment of IE DCs into the small intestine, the expression of MIP-3 α /CCL20, MIP-3 β /

CCL19, RANTES/CCL5, eotaxin/CCL11, MIP-1 α /CCL3, MIP-1 β /CCL4, MCP-1/CCL2, known to attract DCs, was examined first at the RNA level on specimens of intestinal tissues (excluding PP), at different time points after CT treatment. For this purpose, an RPA was performed on RNAs obtained from small intestine samples at different time intervals after CT feeding. As shown in Fig. 3*A*, CCL20/MIP-3 α mRNA levels were markedly increased 1 h after CT treatment and had decreased to almost baseline levels after 6 h. None of the other chemokines transcripts tested were modified by this treatment (data not shown). These results were confirmed at the protein level by ELISA analyses of detergent-treated intestinal specimens processed by the PERFEXT technique. As shown in Fig. 3*B*, a transient increase in CCL20 chemokine content was readily observed in the small intestine 5 h after feeding CT. By 15 h, CCL20 levels had decreased to baseline levels.

Oral administration of CT induces a massive expansion of DCs in draining MLN

DCs from MLN were purified from mice at different time intervals after feeding CT. At 24 h following feeding CT, the total number of DCs recovered from MLN increased by 6-fold (88,000 \pm 21,000 DCs in CT-treated mice vs 15,000 \pm 8,000 DCs in control mice; $n = 7$ experiments). By 48 h, DC numbers in MLN had markedly decreased to near baseline levels (Fig. 2*C*). Furthermore, similar to PP, oral treatment with CT had no effect on spleen DC numbers at all times examined (data not shown).

According to previous studies (10), two DC subsets were identified in MLN, PP, and spleen, based on the differential expression

of CD8 α and CD11b by CD11c⁺ DCs. In addition, a third and most prominent subpopulation with intermediate levels of CD8 α and negative for CD11b was found exclusively in MLN (Fig. 4A). As shown in Fig. 4, feeding mice CT led to a marked increase in the number of CD8^{int} DCs in MLN. Thus, within 24 h after feeding CT, the proportion of CD8^{int} DCs among CD11c⁺ MLN DCs was markedly increased from 43% (corresponding to 7,000 \pm 4,000 CD8^{int} DCs) in control mice to nearly 70% (63,000 \pm 24,000 CD8^{int} DCs per mouse) in CT-treated mice. At 48 h, MLN CD8^{int} DCs returned to control levels. Similarly, but to a lesser extent, the number of CD8⁻ DCs increased in MLN 24 h after feeding CT (4,000 \pm 2,000 DCs per control mouse vs 18,500 \pm 6,000 per CT-treated mouse) and progressively decreased thereafter (Fig. 4B). In contrast, CD8⁺ DC numbers in MLN were not affected by oral administration of CT at all time points examined (Fig. 4B).

To test the hypothesis that the increase of mesenteric CD8^{int} DCs after CT treatment may be due to the recruitment of a blood DC precursor via MLN HEV rather than from lymph-borne DCs, mice were injected with anti-CD62L or anti- $\alpha_4\beta_7$ mAbs, which block migration through MLN HEV (11, 19). We compared the effect of these blocking Abs on DC mobilization into MLN 24 h after CT feeding. Treatment with anti-CD62L and anti- $\alpha_4\beta_7$ Abs *in vivo* had no apparent effect on the increase in CD8^{int} DCs induced by CT, even though it was shown that these Abs were efficient at blocking leukocytes entry via HEV under identical experimental conditions. Thus, in two independent experiments, the frequency of CD8^{int} DCs among MLN DCs from mice pretreated with anti-CD62L and anti- $\alpha_4\beta_7$ Abs and fed CT did not differ from that of mice fed CT but pretreated with isotype-matched control Abs (68 \pm 4%; n = 5 mice per experiment) and is higher than the frequency of unfed control mice (43 \pm 4.5%; n = 5 mice per experiment).

Oral administration of CT enhances the *in vitro* and *in vivo* T cell-stimulatory activity of MLN DCs

DCs were isolated from MLN and PP 24 h after feeding CT, and their ability to stimulate the proliferation of naive TCR transgenic T cells was assessed *in vitro*. Purified naive TCR transgenic T cells expressing the TCR TCR-HA specific for the influenza virus HA immunodominant epitope (aa 110–119) were used. MLN DCs from CT-fed mice were able to prime naive T cells ~3-fold more efficiently than corresponding DCs from control mice (Fig. 5). In contrast, CT feeding had no effect on the T cell-stimulatory activity of DCs from PP (Fig. 5). Interestingly, fractionation of the different MLN DC subsets showed that CD8^{int} and CD8⁻ DCs from CT-fed mice had increased immunostimulatory properties, whereas CD8⁺ DCs remained unaffected by prior CT feeding (Fig. 6A). Moreover, orally administered CT up-regulated the expression of costimulatory molecules CD40, CD80, and CD86 by MLN CD8⁻ and CD8^{int} DCs but only CD40 by CD8⁺ DCs (Fig. 6B).

We have demonstrated that oral administration of CT affects the frequency, phenotype, and immunostimulatory properties of the different MLN DC subsets. This suggested that each of these DC subsets might have different roles in the presentation of Ags orally coadministered with CT. To test this hypothesis, we used an adoptive transfer system to investigate the ability of purified MLN DC subsets isolated from mice fed an Ag coadministered with CT, to prime specific T cells *in vivo*. To perform this experiment, a CTB fusion protein carrying the immunodominant HA peptide (CTB::HA) was fed to groups of BALB/c mice in the presence or absence of CT. After 24 h, the mice were sacrificed, and the MLN were removed. MLN DC subsets were separated and *s.c.* infused into recipient TCR-HA transgenic mice. After 7 days, the popliteal

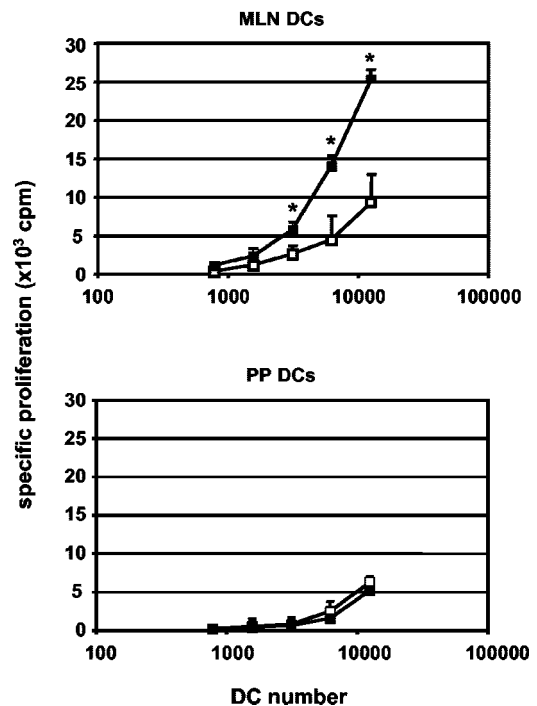


FIGURE 5. Oral administration of CT increases the T cell-stimulatory activity of MLN DCs but not PP DCs. Purified lymph node T cells from naive TCR-HA transgenic mice were cultured *in vitro* with variable numbers of highly enriched MLN DCs or PP DCs isolated from CT-treated (■) or control mice (□) in the presence or absence of HA peptide. Cell proliferation was measured by [³H]thymidine incorporation after an 18-h pulse at the end of a 4-day proliferation assay. Data represent mean numbers of counts per minute (\pm SD) determined on three independent groups per condition and are representative of two separate experiments. *, Statistical difference (p < 0.05; Student-Newman-Keuls test).

draining lymph nodes were excised, and the frequency of TCR-HA⁺CD4⁺ T cells was analyzed by flow cytometry.

As shown in Fig. 7, transfer of CD8^{int} DCs after feeding with CTB::HA and CT increased the number of TCR-HA⁺CD4⁺ T cells in the draining lymph node of recipient mice by a factor of 3 compared with control mice, which received CD8^{int} DCs from donors fed with CTB::HA alone. Similar results were obtained for the CD8⁻ subset, whereas infusion of CD8⁺ DC had no apparent effect.

Distinct subsets of MLN DCs promote priming for Th2 responses after oral administration of CT

The influence of MLN DCs on the capacity of CT to induce the differentiation of naive TCR-HA⁺CD4⁺ T cells was examined *in vitro*. MLN DCs were isolated 24 h after feeding CT. DC subsets were purified and cultured with TCR-HA⁺CD4⁺ transgenic T cells and HA peptide. After 48 h, T cells were harvested, washed, and allowed to rest for an additional 4 days in the absence of HA peptide. Subsequently, T cell cultures were restimulated with HA-pulsed syngeneic spleen cells, and supernatants from secondary cultures were assayed for Th1 and Th2 cytokine contents. As shown in Table I, prior priming of TCR-HA T cells by MLN CD8^{int} and CD8⁻ DCs from mice fed CT led to increased IL-4 production in secondary cultures as compared with CD8⁺ MLN DCs and with corresponding DC subsets from control mice. IFN- γ production was comparable between all experimental groups. Thus, CD8^{int} and CD8⁻ MLN DCs appear to promote the preferential differentiation of naive CD4⁺ T cells into Th2 cells.

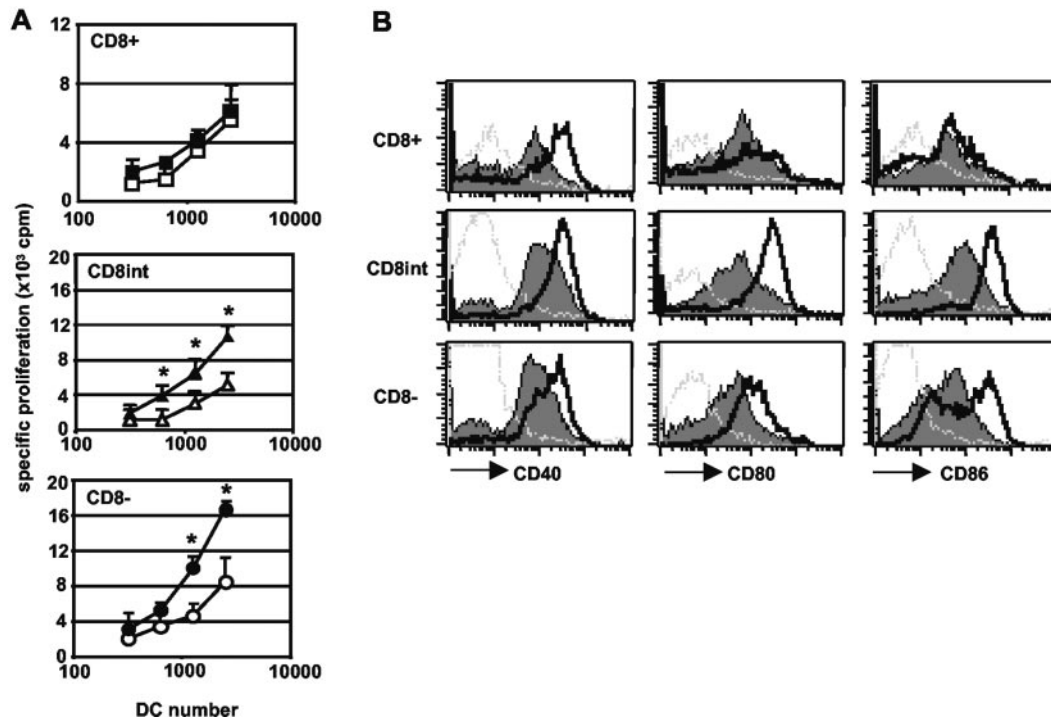


FIGURE 6. Oral administration of CT potentiates the immunostimulatory properties of MLN CD8^{int} and CD8⁻ MLN DC subsets. *A*, Purified lymph node T cells from naive TCR-HA transgenic mice were cultured in vitro with graded numbers of highly enriched MLN DC subsets isolated from CT-treated (■, ▲, ●) or control mice (□, △, ○) in the presence or absence of HA peptide. MLN DC subsets correspond to sorted CD8⁺CD11c⁺ DCs (CD8⁺; ■, □), gated CD8^{int}CD11c⁺ DCs (CD8^{int}; ▲, △), and gated CD8⁻CD11c⁺ DCs (CD8⁻; ●, ○) obtained after triple staining using FITC-conjugated anti-CD11c, PE-conjugated anti-CD8 α , and tricolor-conjugated CD11b. Cell proliferation was measured by [³H]thymidine incorporation after an 18-h pulse at the end of a 4-day proliferation assay. Data are expressed as mean (+SD) numbers of counts per minute from samples analyzed in triplicate and are representative of two individual experiments with similar results. *, Statistical difference ($p < 0.05$; Student-Newman-Keuls test). *B*, Costimulatory molecule expression by MLN DC subsets was analyzed by flow cytometry. Histograms correspond to costimulatory molecule expression by gated CD8⁺, CD8^{int}, and CD8⁻ MLN CD11c⁺ DC subsets from mice 24 h after feeding CT (black bold line) and from unfed mice (filled histograms). Gray lines correspond to background staining with isotype-matched mAbs. These data are representative of three independent experiments.

Discussion

This study demonstrates that oral administration of the mucosal adjuvant CT induces the sequential expansion of DCs in the subepithelial mucosa of small intestinal villi and in draining MLN, without affecting DC cellularity in PP. Importantly, oral CT enhanced the immunostimulatory activity of MLN DCs but had apparently no such effect on PP DCs. Thus, CT may exert its adjuvant activity by attracting DCs toward the mucosal epithelium and by stimulating their maturation as they subsequently migrate to the MLN.

The CD11c⁺CD8 α ⁻ DCs identified beneath the epithelium of small intestinal villi appear to represent a relatively immature DC population whose phenotype resembles epidermal LCs. In contrast to PP CD11c⁺CD8 α ⁻ DCs located in the subepithelial area of the dome (20, 21), intestinal DCs express the DEC-205 Ag, but comparatively low levels of costimulatory molecules CD80 and CD86, and like LCs can be mobilized by CT (22). Thus, CD8⁻ PP DCs and intestinal DCs appear to represent separate subsets or originate from the same DC precursor but at different stages of maturation (10, 20, 21). Furthermore, and akin to intestinal intraepithelial lymphocytes (23), intestinal DCs express the integrin $\alpha_E\beta_7$ (CD103) but neither L-selectin nor $\alpha_4\beta_7$, and thus seem to be destined to the gut epithelium, which expresses E-cadherin, the receptor for $\alpha_E\beta_7$ (24). This likely explains why intestinal DCs could be released readily by simple dispersion of the intestinal epithelium and suggests that these immature DCs resemble or comprise a subpopulation of dendritic-like cells described earlier in the rat intestinal epithelium (25). These CD8⁻, CD11b⁺,

CD11c⁺ DCs differ from the CD8⁻, CD11c⁺ cells recently identified in the murine lamina propria (26), which do not express CD11b. Although we could not detect such cells, probably due to the use of different staining Abs, we cannot rule out the possibility that the IE DCs identified in our study represent a contingent of cells derived from lamina propria DCs.

The observation that oral CT induced a very rapid mobilization of immature CD11c⁺CD8 α ⁻ DCs in the subepithelial area of small intestinal villi could be explained by the fact that such treatment selectively induced the production of CCL20/MIP-3 α in the gut. This chemokine has recently been shown to be produced by intestinal epithelial cells and to attract immature blood-derived DCs in vitro in response to *Salmonella typhi* flagellin (27), which is an adjuvant in vivo (28). Together, these observations underline the role of the intestinal epithelium in promoting the immunopotentiating activity of mucosal adjuvants.

The early but transient recruitment of CD11c⁺CD8⁻ DCs induced by oral CT in the small intestine was rapidly followed by a massive accumulation of CD11c⁺ DCs in draining MLN, but not in PP and in the spleen. Of the three major DC subsets isolated from MLN, oral treatment with CT preferentially increased the numbers of the CD8^{int} DC subset and to a lesser extent CD8⁻ DC numbers. Furthermore, both MLN DC subsets displayed enhanced expression of the costimulatory molecules CD80 and CD86 upon oral CT treatment, in keeping with the recently reported in vitro effects of CT on human blood-derived and murine bone marrow-derived DCs (29–31). These findings suggest that CT not only induces recruitment and migration of mucosal DCs but can also

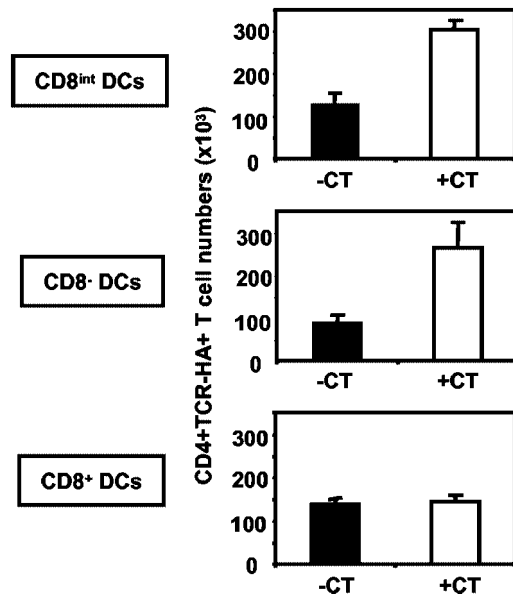


FIGURE 7. Oral coadministration of CT and Ag enhances the T cell stimulatory activity of CD8^{int} and CD8⁻ MLN DC subsets in vivo. MLN DC subsets (CD8⁺, CD8^{int}, and CD8⁻) were isolated from mice 24 h after feeding either CTB-HA (■) or CTB-HA and CT (□). Highly enriched DC subsets (50,000) were transferred s.c. to TCR-HA transgenic mice. The frequency of CD4⁺TCR-HA⁺ T cells in the draining lymph nodes of recipient mice was determined 7 days after DC adoptive transfer by FACS analysis. Data represent the mean (+SEM) of two independent experiments.

promote their maturation in vivo. Because in vivo blockade of L-selectin and $\alpha_4\beta_7$ integrin, a treatment effective for preventing entry of blood leukocytes into MLN (11, 19), failed to interfere with the expansion of CD8^{int} DCs in MLN, these cells do not appear to originate from a blood precursor or use alternative mechanisms to enter MLN. MLN CD8^{int} DCs thus likely represent recent migrants derived from immature DCs in the intestinal mucosa that enter MLN while maturing. This hypothesis is compatible with our previous data showing that peripheral lymph node CD8^{int} DCs represent recent emigrants from the skin (10) and constitute a mature stage of LCs (32). Therefore, it is tempting to speculate that immature CD8⁻CD11c⁺ DCs identified in this study are the mucosal equivalent of epidermal LCs and can capture luminal Ags independently of PP M cells. This explanation is supported by an in vitro study by Rescigno et al. (33), which suggested that DCs opened tight junctions between epithelial cells to directly pick up Ags in the intestine lumen.

The ability of oral CT to enhance the stimulatory properties of the CD8^{int} and CD8⁻ MLN DCs on naive T cells in vitro as well as in vivo, in addition to dramatically increasing their frequencies, further underscores the role of these DC subsets in the induction of intestinal immune responses. Given the apparent lack of effects of CT on PP DC cellularity and T cell-stimulatory activity, the results of this study strongly suggest that MLN DCs rather than PP DCs play a critical role in the adjuvanticity of CT on gut mucosal immune responses. The latter interpretation is also consistent with earlier studies indicating that PP may not be required for the induction of secretory and systemic T cell responses to fed Ags (34, 35). Furthermore, results from adoptive transfer experiments demonstrated that the very same MLN DC subsets could acquire an Ag orally coadministered with CT. Moreover, the ability of MLN DC subsets to promote the differentiation of naive CD4⁺ T cells in Th2 cells are consistent with previous reports showing that CT prefer-

Table I. Oral CT promotes priming of CD4⁺ T cells for Th2 responses by MLN DCs^a

MLN DC priming	Cytokine Production (pg/ml)	
	IFN- γ	IL-4
CTRL CD8 ⁺ DCs	49	<12
CT CD8 ⁺ DCs	45	<12
CTRL CD8 ^{int} DCs	44	<12
CT CD8 ^{int} DCs	45	300
CTRL CD8 ⁻ DCs	50	<12
CT CD8 ⁻ DCs	45	544

^a MLN DC subsets from mice fed CT or from control mice were cultured with CD4⁺TCR-HA⁺ T cells and HA peptide. After 48 h, cells were harvested and allowed to rest during a period of 4 days and then cultured with HA-pulsed syngeneic spleen cells. After 48 h, supernatants from these secondary cultures were assayed for cytokine content by ELISA. These data are representative of two independent experiments. CTRL, Control.

entially promotes Th2 responses to orally administered Ags (6) and can induce monocyte-derived blood DCs to favor the differentiation of naive T cells toward the Th2 phenotype (29). Together with the fact that CT not only enhances mucosal and systemic immune responses but also abrogates peripheral tolerance to orally coadministered Ags (3), this study lend support to the notion that specialized subpopulations of mucosal DCs play a critical role in the control of immune responsiveness in the gut.

Acknowledgments

We thank Dr. B. Ferrua (Groupe de Recherche en Immunopathologie de la Leishmaniose, Faculty of Medicine, Nice, France) for helpful advice. We gratefully acknowledge Thierry Juhel, Valérie Milcent, and Gun Walleström for expert technical assistance, and Dr. J. P. Breittmayer (Institut National de la Santé et de la Recherche Médicale, Unité 343, Nice, France) for performing cell sortings.

References

- Czerkinsky, C., F. Anjuere, J. R. McGhee, A. George-Chandy, J. Holmgren, M.-P. Kiény, K. Fujiyashi, J. Mestecky, V. Pierrefite-Carle, C. Rask, and J. B. Sun. 2000. Mucosal immunity and tolerance: relevance to vaccine development. *Immunol. Rev.* 170:197.
- Weiner, H. L. 2000. Oral tolerance, an active immunologic process mediated by multiple mechanisms. *J. Clin. Invest.* 106:935.
- Elson, C. O., and W. Ealding. 1984. Cholera toxin feeding did not induce oral tolerance in mice and abrogated oral tolerance to an unrelated protein antigen. *J. Immunol.* 133:2892.
- Holmgren, J., N. Lycke, and C. Czerkinsky. 1993. Cholera toxin and cholera B subunit as oral-mucosal adjuvant and antigen vector systems. *Vaccine* 11:1179.
- Lycke, N., and J. Holmgren. 1986. Strong adjuvant properties of cholera toxin on gut mucosal immune responses to orally presented antigens. *Immunology* 59:301.
- Xu-Amano, J., H. Kiyono, R. J. Jackson, H. F. Staats, K. Fujihashi, P. D. Burrows, C. O. Elson, S. Pillai, and J. R. McGhee. 1993. Helper T cell subsets for immunoglobulin A responses: oral immunization with tetanus toxoid and cholera toxin as adjuvant selectively induces Th2 cells in mucosa associated tissues. *J. Exp. Med.* 178:1309.
- Holmgren, J. 1981. Actions of cholera toxin and the prevention and treatment of cholera. *Nature* 292:413.
- Steinman, R. M., and M. C. Nussenzweig. 2002. Avoiding horror autotoxicus: the importance of dendritic cells in peripheral T cell tolerance. *Proc. Natl. Acad. Sci. USA* 99:351.
- Banchereau, J., F. Briere, C. Caux, J. Davoust, S. Lebecque, Y. T. Liu, B. Pulendran, and K. Palucka. 2000. Immunobiology of dendritic cells. *Annu. Rev. Immunol.* 18:767.
- Anjuere, F., P. Martín, I. Ferrero, M. López, G. Martínez del Hoyo, N. Wright, and C. Ardavin. 1999. Definition of dendritic cell subpopulations present in the spleen, Peyer's patches, lymph nodes and skin of the mouse. *Blood* 93:590.
- Martin, P., S. Ruiz Ruiz, G. M. del Hoyo, F. Anjuere, H. Hernandez Vargas, M. Lopez-Bravo, and C. Ardavin. 2002. Dramatic increase in lymph node dendritic cell number during infection by the mouse mammary tumor virus occurs by CD62L-dependent blood-borne DC recruitment. *Blood* 99:1282.
- O'Connell, P. J., Y. I. Son, A. Giermasz, Z. Wang, A. J. Logar, A. W. Thomson, and P. Kalinski. 2003. Type-1 polarized nature of mouse liver CD8 α ⁻ and CD8 α ⁺ dendritic cells: tissue-dependent differences offset CD8 α -related dendritic cell heterogeneity. *J. Immunol.* 170:2007.
- Kirberg, J., A. Baron, S. Jakob, A. Rolink, K. Karjalainen, and H. Von Boehmer. 1994. Thymic selection of CD8⁺ single positive cells with a class II major histocompatibility complex-restricted receptor. *J. Exp. Med.* 180:25.

14. Lebens, M., S. Johansson, J. Osek, M. Lindblad, and J. Holmgren. 1993. Large-scale production of *Vibrio cholerae* toxin B subunit for use in oral vaccines. *Biotechnology* 11:1574.
15. Witholt, B., M. Boekhout, M. Brock, J. Kingma, H. V. Heerikhuizen, and W. Leisgang. 1976. An efficient and reproducible procedure for the formation of spheroplasts from variously grown *Escherichia coli*. *Anal. Biochem.* 74:160.
16. Anjuère, F., and C. Ardavin. 2001. Isolation of mouse thymic dendritic cells. In *Dendritic Cell Protocols*. S. Robinson and A. Stagg, eds. Humana, Totowa, NJ, p. 23.
17. Becksteadt, J. M. 1994. A simple technique for preservation of fixation-sensitive antigens in paraffin-embedded tissues. *J. Histochem. Cytochem.* 42:737.
18. Villavedra, M., H. Carol, M. Hjulstrom, J. Holmgren, and C. Czerkinsky. 1997. PERFEXT: a direct method for quantitative assessment of cytokine production in vivo at the local level. *Res. Immunol.* 148:257.
19. Hamann, A., D. P. Andrew, D. Jablonski-Westrich, B. Holzmann, and E. Butcher. 1994. Role of α_4 -integrins in lymphocyte homing to mucosal tissues in vivo. *J. Immunol.* 152:3282.
20. Ruedl, C., C. Rieser, G. Böck, G. Wick, and H. Wolf. 1996. Phenotypic and functional characterization of CD11c⁺ dendritic cell population in mouse Peyer's patches. *Eur. J. Immunol.* 26:1801.
21. Kelsall, B. L., and W. Strober. 1996. Distinct populations of dendritic cells are present in the subepithelial dome and T cell regions of the murine Peyer's patch. *J. Exp. Med.* 183:237.
22. Anjuère, F., A. George-Chandy, F. Audant, D. Rousseau, J. Holmgren, and C. Czerkinsky. 2003. Transcutaneous immunization with cholera toxin B subunit adjuvant suppresses IgE antibody responses via selective induction of Th1 immune responses. *J. Immunol.* 170:1586.
23. Kilshaw, P. J., and S. J. Murrant. 1991. Expression and regulation of $\beta_7(\beta_7)$ integrins on mouse lymphocytes: relevance to the mucosal immune system. *Eur. J. Immunol.* 21:2591.
24. Cepek, K. L., S. K. Shaw, C. M. Parker, G. J. Russell, J. S. Morrow, D. L. Rimm, and M. D. Brenner. 1994. Adhesion between epithelial cells and T lymphocytes mediated by E-cadherin and the $\alpha_E\beta_7$ integrin. *Nature* 372:190.
25. Maric, I., P. G. Holt, M. H. Perdue, and J. Bienenstock. 1996. Class II MHC antigen (Ia)-bearing dendritic cells in the epithelium of the rat intestine. *J. Immunol.* 15:1408.
26. Becker, C., S. Wirtz, M. Blessing, J. Pirhonen, D. Strand, O. Bechthold, J. Frick, P. R. Galle, I. Autenrieth, and M. F. Neurath. 2003. Constitutive p40 promoter activation and IL-23 production in the terminal ileum mediated by dendritic cells. *J. Clin. Invest.* 112:693.
27. Sierro, F., B. Dubois, A. Coste, D. Kaiserlian, J. P. Kraehenbuhl, and J. C. Sirard. 2001. Flagellin stimulation of intestinal epithelial cells triggers CCL20-mediated migration of dendritic cells. *Proc. Natl. Acad. Sci. USA* 98:13722.
28. McSorley, S. J., B. D. Ehst, Y. Yu, and A. T. Gewirtz. 2002. Bacterial flagellin is an effective adjuvant for CD4⁺ T cells in vivo. *J. Immunol.* 169:3914.
29. Gagliardi, M. C., F. Sallusto, M. Marinaro, A. Langenkamp, A. Lanzavecchia, and M. T. De Magistris. 2000. Cholera toxin induces maturation of human dendritic cells and licenses them for Th2 priming. *Eur. J. Immunol.* 30:2394.
30. George-Chandy, A., K. Eriksson, M. Lebens, I. Nordstrom, E. Schon, and J. Holmgren. 2001. Cholera toxin B subunit as a carrier molecule promotes antigen presentation and increases CD40 and CD86 expression on antigen-presenting cells. *Infect. Immun.* 69:5716.
31. Lavelle, E. C., E. McNeela, M. E. Armstrong, O. Leavy, S. C. Higgins, and K. H. Mills. 2003. Cholera toxin promotes the induction of regulatory T cells specific for bystander antigens by modulating dendritic cell activation. *J. Immunol.* 171:2384.
32. Anjuère, F., G. Martinez del Hoyo, P. Martín, and C. Ardavin. 2000. Langerhans cells acquire a CD8⁺ dendritic cell phenotype upon maturation by CD40 ligation. *J. Leukocyte Biol.* 67:206.
33. Rescigno, M., M. Urbano, B. Valzasina, M. Francolini, G. Rotta, R. Bonasio, F. Granucci, J.-P. Kraehenbuhl, and P. Ricciardi-Castagnoli. 2001. Dendritic cells express tight junction proteins and penetrate gut epithelial monolayers to sample bacteria. *Nat. Immunol.* 2:361.
34. Yamamoto, M., P. Rennert, J. R. McGhee, M. N. Kweon, S. Yamamoto, T. Dohi, S. Otake, H. Bluethmann, K. Fujihashi, and H. Kiyono. 2000. Alternate mucosal immune system: organized Peyer's patches are not required for IgA responses in the gastrointestinal tract. *J. Immunol.* 164:5184.
35. Alpan, O., G. Rudomen, and P. Matzinger. 2001. The role of dendritic cells, B cells, and M cells in gut-oriented immune responses. *J. Immunol.* 166:4843.